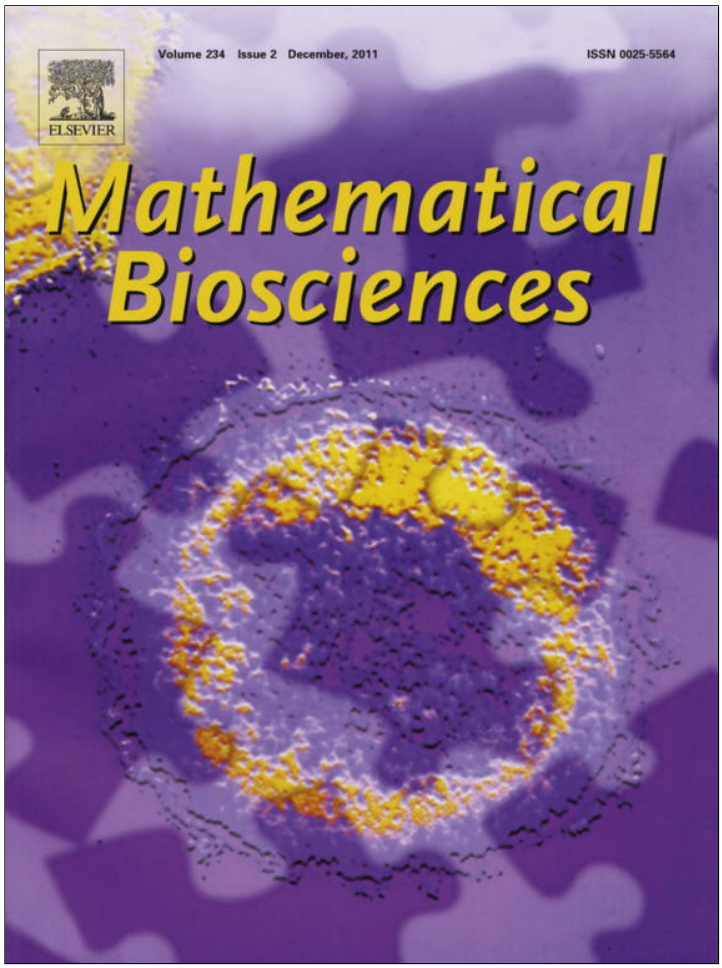

Mathematical Biosciences 234 (2011) 95–107

Contents lists available at SciVerse ScienceDirect

Mathematical Biosciences

journal homepage: www.elsevier.com/locate/mbs

Dynamics and bifurcation of a model for hormonal control of the menstrual cycle with inhibin delay ☆

Alison Margolskee [a], James F. Selgrade [b,*]

[a] Department of Mathematics, North Carolina State University, Raleigh, NC 27695-8205, United States
[b] Department of Mathematics and Biomathematics Program, North Carolina State University, Raleigh, NC 27695-8205, United States

ARTICLE INFO

Article history:
Received 18 May 2011
Received in revised form 31 August 2011
Accepted 2 September 2011
Available online 14 September 2011

Keywords:
Estradiol
Follicle
Hill function
Degenerate Hopf bifurcation

ABSTRACT

A system of 13 ordinary differential equations with 42 parameters is presented to model hormonal regulation of the menstrual cycle. For an excellent fit to clinical data, the model requires a 36 h time delay for the effect of inhibin on the synthesis of follicle stimulating hormone. Biological and mathematical reasons for this delay are discussed. Bifurcations with respect to changes in three important parameters are examined. One parameter represents the level of estradiol adequate for significant synthesis of luteinizing hormone. Bifurcation diagrams with respect to this parameter reveal an interval of parameter values for which a unique stable periodic solution exists and this solution represents a menstrual cycle during which ovulation occurs. The second parameter measures mass transfer between the first two stages of ovarian development and is indicative of healthy follicular growth. The third parameter is the time delay. Changes in the second parameter and the time delay affect the size of the uniqueness interval defined with respect to the first parameter. Saddle-node, transcritical and degenerate Hopf bifurcations are studied.

1. Introduction

Systems of ordinary and delayed differential equations have been used to model hormonal regulation of the human menstrual cycle, e.g., see Bogumil et al. [4,5], McIntosh and McIntosh [20], Plouffe and Luxenberg [25], Selgrade and Schlosser [36], Schlosser and Selgrade [32], Harris-Clark et al. [14], Reinecke and Deuflhard [27], and Pasteur [24]. Dual control of the menstrual cycle depends on hormones produced by the hypothalamus and the pituitary glands in the brain and by the ovaries. The pituitary prompted by signals from the hypothalamus secretes follicle stimulating hormone (*FSH*) and luteinizing hormone (*LH*) which control ovarian development and ovulation, see [15,41,42]. The ovaries produce estradiol (E_2), progesterone (P_4) and inhibin (*Inh*) which affect the synthesis and release of *FSH* and *LH*, see [16,19,38]. Harris-Clark et al. [14], Pasteur [24], Schlosser and Selgrade [32], and Selgrade and Schlosser [36] have derived a 13-dimensional system of delayed differential equations which captures these interacting mechanisms. Model parameters were identified using two different clinical data sets for normally cycling women [21,39]. Model simulations with parameters from the McLachlan data [21] revealed two stable periodic solutions [14] – one fitting the McLachlan data for normally cycling women and the other being non-ovulatory because of no *LH* surge. The non-ovulatory cycle has similarities to an abnormal cycle of a woman with polycystic ovarian syndrome (PCOS) [40], the leading cause of female infertility. However, model simulations corresponding to the Welt parameters produced only one stable periodic solution and it fits the Welt data for normally cycling women. Selgrade et al. [35] explained this apparent inconsistency by showing that a change in only one sensitive parameter of the Welt system would result in the Welt model exhibiting bistability like the McLachlan model.

Abnormal cycling and non-ovulatory cycling have serious health and reproductive consequences. In fact, between 6% and 9% of adult women exhibit some symptoms of PCOS, see Azziz et al. [2], and Alvarez-Blasco et al. [1]. Since cycle irregularities are usually associated with abnormal hormone levels, mathematical models of hormonal regulation may provide information about parameter variations which result in abnormal cycling and may provide insights about possible hormonal therapies. In an effort to understand what parameter ranges result in normal and abnormal cycling, Selgrade [34] set the time-delays to zero in the Welt model and used the software XPPAUT [9] to study bifurcation diagrams with respect to two of the most sensitive parameters. Bifurcation diagrams for the resulting autonomous system could be drawn with the features of AUTO [7] in XPPAUT. This autonomous model gives an acceptable fit to the 28 day Welt data set [39]

☆ Research supported by NSF Grant DMS-0920927.
* Corresponding author. Tel.: +1 919 515 8589; fax: +1 919 515 3798.
E-mail addresses: amargol@ncsu.edu (A. Margolskee), selgrade@math.ncsu.edu (J.F. Selgrade).

0025-5564/$ - see front matter © 2011 Elsevier Inc. All rights reserved.
doi:10.1016/j.mbs.2011.09.001

except some hormone peaks are lower than the data and the period for the normal cycle is only about 26 days, see Fig. 1.

Based on model sensitivity analysis [24,35], the two key parameters for study in [34] were Km_{LH} and c_2. Km_{LH} is the half-saturation constant which represents the level of E_2 sufficient for significant *LH* synthesis and the *LH* surge. c_2 indicates the ovarian mass transfer rate between the first two stages of ovarian development. The bifurcation diagram with respect to Km_{LH} reveals an interval of Km_{LH} parameter values for which a unique stable periodic solution exists and this solution represents a menstrual cycle with an *LH* surge adequate for ovulation. If Km_{LH} lies outside this cycle uniqueness interval then either no *LH* surge occurs or there are two stable cycles – one is ovulatory and the other may be non-ovulatory because of an insufficient *LH* surge. Changes in c_2 affect the size of this interval because of the positions of Hopf, saddle-node and transcritical bifurcations as discussed in [34].

In this study, we carry out a bifurcation analysis for the system of delayed differential equations using the DDEBIFTOOL [8], which is designed to handle the delay. The original model [14] had three discrete time-delays (one corresponding to each ovarian hormone) which represented the time interval between changes in ovarian hormone concentrations and subsequent changes they cause in synthesis rates of the pituitary hormones. Here we show that including only a delay of $\tau = 1.5$ days for the effect of the peptide inhibin on the pituitary's secretion of *FSH* improves the fit to the Welt data (see Fig. 1) and this time lag in the effect of inhibin is consistent with observations from experiments with rhesus monkeys [26]. The other two delays, which pertain to the steroids E_2 and P_4, were less than a day and did not contribute significant additional improvement. So they are set to zero for this study. The system with the inhibin delay has larger uniqueness intervals than the model with no delay (see Table 2). Hence, an inhibin delay may enhance the possibility of ovulation. In Section 3 we speculate about the biological reasons for this improvement in model behavior due to inhibin delay. We examine bifurcation diagrams with respect to Km_{LH} for the delayed system and show that the cycle uniqueness interval is usually determined by two saddle-node bifurcations. For the delay τ fixed at 1.5 days, we illustrate how this interval may be enlarged by varying c_2 due to the occurrence of two degenerate Hopf bifurcations. Then for fixed c_2, we increase the delay parameter τ from 0 to 1.5 to unfold transcritical bifurcations and produce large cycle uniqueness intervals. Finally, we illustrate how loops in the Km_{LH} bifurcation diagrams may appear and disappear by varying the parameters τ and c_2.

2. Biological background and model equations

The menstrual cycle for an adult female consists of the follicular phase, ovulation, the luteal phase and menstruation (e.g., see Odell [22] or Ojeda [23]). Pulses of gonadotropin-releasing hormone (*GnRH*) produced by the hypothalamus modulate pulses of *FSH* and *LH* secreted by the pituitary. These pulses are on a time scale of minutes but, because the ovaries respond to average daily blood levels [22], our model tracks average daily concentrations of *FSH* and *LH*. Hence we lump the effects of the hypothalamus and the pituitary together and just consider the synthesis and release of

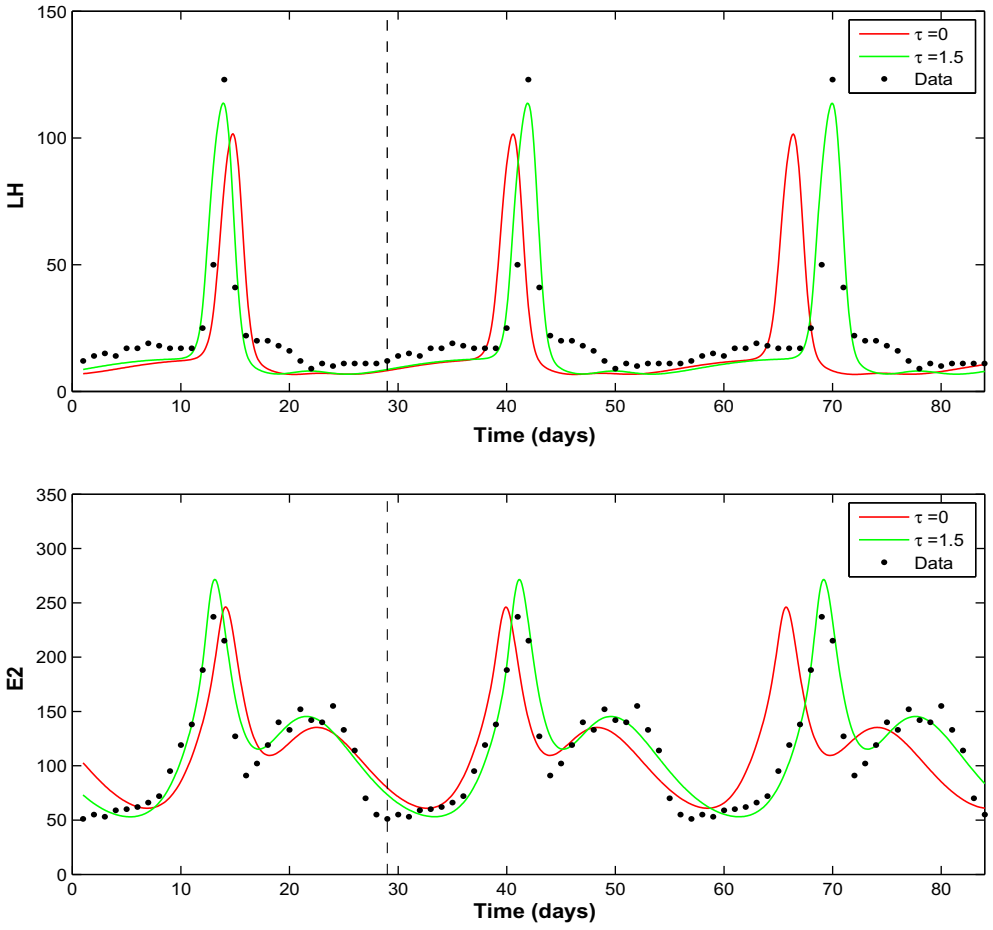

Fig. 1. *LH* and E_2 simulations for three cycles of the Welt model with inhibin delay τ of 1.5 days (green curves) and no delay (red curves) with data points (84 black dots) corresponding to the 28 day data from Welt et al. [39] plotted three times. The vertical dashed line indicates day 29, where the second cycle begins and where both solution orbits are very close to one another.

FSH and *LH* on the time scale of days. This simplification results in a model which gives good fit to the daily data of Welt et al. [39] and which avoids the complication of multiple time scales.

During the follicular phase, *FSH* produced by the pituitary gland promotes the development of 6–12 follicles. Typically one dominant follicle is selected to grow to maturity and to produce a large amount of E_2 which primes the pituitary for *LH* secretion. At mid-cycle, a surge of *LH* over a period of 4 or 5 days results in ovulation. After releasing its ovum, the dominant follicle becomes the corpus luteum which produces hormones in preparation for pregnancy and produces P_4 and *Inh* which inhibit *LH* and *FSH*, respectively. If fertilization does not occur, the corpus luteum atrophies, menstruation follows and a rise in *FSH* marks the beginning of the next cycle.

Harris [13], Harris-Clark et al. [14], Pasteur [24], Schlosser and Selgrade [32], and Selgrade and Schlosser [36] developed a model for this endocrine control system based on 13 ordinary differential equations (S) with three auxiliary equations (A) and with discrete time delays. Four of these differential equations (S1)–(S4) describe the synthesis, release and clearance of *LH* and *FSH*. The state variables RP_{LH} and RP_{FSH} represent the amounts of these hormones in the pituitary and *LH* and *FSH* represent the blood concentrations of these hormones. The biological literature (e.g., [16,19,41]) indicates that *LH* exhibits a biphasic response to E_2. To capture this our model assumes that the effect of E_2 on *LH* synthesis is different than the effect on *LH* release, i.e., E_2 inhibits release (see the denominator of the second term in (S1)) but at high levels E_2 promotes synthesis (see the Hill function in the numerator of the first term of (S1)). On the other hand, P_4 inhibits *LH* synthesis but promotes release. The release term appears in (S1) as a decay term and in (S2) as a growth term, where it is divided by blood volume v. Equations (S3) and (S4) for *FSH* are similar except the synthesis term has Inh inhibition which is delayed by time τ. The parameters in (S1)–(S4) are named according to the traditional usage for chemical reactions, e.g., $V_{1,LH}$ denotes the velocity of the reaction (see Keener and Sneyd [17]).

The state variables in (S5)–(S13) represent tissue masses of nine distinct stages of the ovary during the follicular and luteal phases of the cycle. *ReF*, *SeF* and *PrF* denote the recruited follicles, the secondary follicles and the preovulatory or dominant follicle, respectively. Ov_1 and Ov_2 represent periovulatory stages and Lut_i, $i = 1, \ldots, 4$, denote four luteal stages. *LH* and *FSH* promote tissue growth within a stage and the transformation of tissue from one stage to the next. Since clearance from the blood of the ovarian hormones is on a fast time scale, we assume that blood levels of E_2, P_4, and *Inh* are at quasi-steady state [17] as did Bogumil et al. [4]. Hence, we take these concentrations to be proportional to the tissue masses during the appropriate stages of the cycle giving the three auxiliary equations (A1)–(A3) for the ovarian hormones. Here we study the 13-dimensional system (S) with (A), which has one time delay τ. Forty-two parameters are listed in Table 1 and correspond to those which Selgrade [34] used to analyze bifurcation diagrams for the Welt system with time delay set to zero.

System (S) and (A) with the parameters in Table 1 has a stable periodic solution of period 28 days and this solution represents an ovulatory menstrual cycle. This periodic solution gives a very good approximation (see Fig. 1) to the 28 day data set of Welt et al. [39] which contains daily average hormone values computed from blood samples of 23 normally cycling women ranging in age from 20 to 34 years. Because of various intrinsic and extrinsic factors, it is highly unlikely that the cycle length of an individual woman will be always 28 days or that her cycle will be exactly periodic even for a short span of time. The extensive study of Treloar et al. [37] indicated wide variation in inter-person and intra-person cycle length. In fact, a recent dynamical systems analysis [6] of cycle length data over a 20 year span suggested that the menstrual cycle should be described by a chaotic dynamical system. Also, apparent quasi-periodic behavior [31] has been exhibited by a model for the bovine estrous cycle [3], which has some structural similarities to our system. In spite of this variability, Treloar et al. [37] concluded that the "menstrual interval for many persons and covering a wide span of chronologic age should, however, be expected to average within a few days of the oft-quoted 28."

Table 1
Parameters and values for system (S) and auxiliary equations (A).

Eqs. (S1)–(S4)			
τ	1.5 days		
k_{LH}	2.42 day^{-1}		
a_{LH}	14.0 day^{-1}		
$V_{0,LH}$	500 IU/day		
$V_{1,LH}$	4500 IU/day		
Km_{LH}	200 pg/mL		
$Ki_{LH,P}$	12.2 ng/mL		
$c_{LH,E}$	0.004 mL/pg		
$c_{LH,P}$	0.26 mL/ng		
V_{FSH}	375 IU/day		
a_{FSH}	8.21 day^{-1}		
k_{FSH}	1.90 day^{-1}		
$c_{FSH,E}$	0.0018 mL^2/pg^2		
$Ki_{FSH,Inh}$	3.5 IU/mL		
$c_{FSH,P}$	12.0 mL/ng		
v	2.50 L		
Eqs. (S5)–(S13)			
b	0.05 L μg/(IU day)		
c_1	0.08 L/(IU day)		
c_2	0.07 $(L/IU)^{\alpha}$/day		
c_3	0.13 $(L/IU)^{\beta}$/day		
c_4	0.027 L/(IU day)		
c_5	0.51 $(L/IU)^{\gamma}$/day		
d_1	0.50 day^{-1}		
d_2	0.56 day^{-1}		
k_1	0.55 day^{-1}		
k_2	0.69 day^{-1}		
k_3	0.85 day^{-1}		
k_4	0.85 day^{-1}		
α	0.79		
β	0.16		
γ	0.02		
Eqs. (A)			
e_0	30 pg/mL	p_2	0.048 kL^{-1}
e_1	0.11 L^{-1}	h_0	0.4 IU/mL
e_2	0.21 L^{-1}	h_1	0.009 IU/(μg mL)
e_3	0.45 L^{-1}	h_2	0.029 IU/(μg mL)
p_0	0 ng/mL	h_3	0.018 IU/(μg mL)
p_1	0.048 kL^{-1}		

Auxiliary equations (A)

$$E_2 = e_0 + e_1\, SeF + e_2\, PrF + e_3\, Lut_4, \tag{A1}$$

$$P_4 = p_0 + p_1\, Lut_3 + p_2\, Lut_4, \tag{A2}$$

$$Inh = h_0 + h_1\, PrF + h_2\, Lut_2 + h_3\, Lut_3, \tag{A3}$$

System (S)

$$\frac{d}{dt}RP_{LH} = \frac{V_{0,LH} + \frac{V_{1,LH}E_2^8}{Km_{LH}^8 + E_2^8}}{1 + P_4/Ki_{LH,P}} - \frac{k_{LH}[1 + c_{LH,P}P_4]RP_{LH}}{1 + c_{LH,E}E_2}, \tag{S1}$$

$$\frac{d}{dt}LH = \frac{1}{v}\frac{k_{LH}[1 + c_{LH,P}P_4]RP_{LH}}{1 + c_{LH,E}E_2} - a_{LH}LH, \tag{S2}$$

$$\frac{d}{dt}RP_{FSH} = \frac{V_{FSH}}{1 + Inh(t-\tau)/Ki_{FSH,Inh}} - \frac{k_{FSH}[1 + c_{FSH,P}P_4]RP_{FSH}}{1 + c_{FSH,E}E_2^2}, \tag{S3}$$

$$\frac{d}{dt}FSH = \frac{1}{v}\frac{k_{FSH}[1 + c_{FSH,P}P_4]RP_{FSH}}{1 + c_{FSH,E}E_2^2} - a_{FSH}FSH, \tag{S4}$$

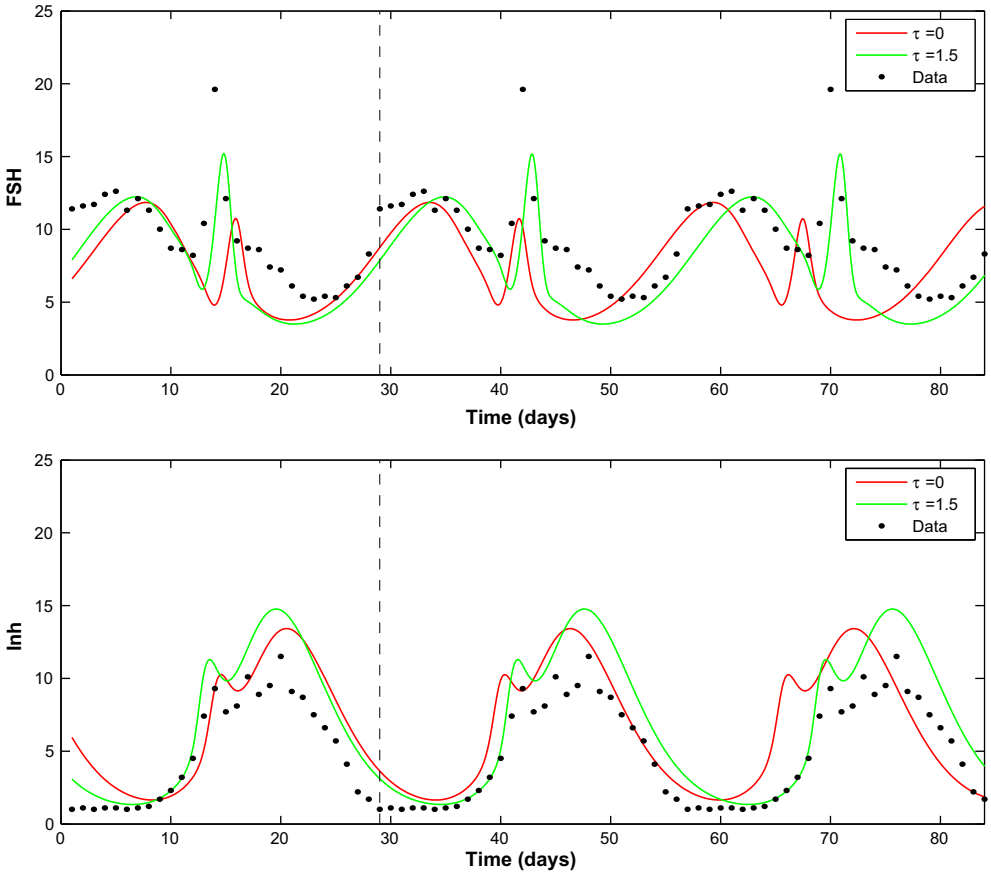

Fig. 2. *FSH* and *Inh* simulations for three consecutive cycles of the delay model (green curves) and the no delay model (red curves) with 84 data points [39]. The vertical dashed line indicates day 29, the beginning of the second cycle. From day 14.5 to day 33.5 the synthesis of delay *FSH* is suppressed more than the synthesis of no delay *FSH* because of inhibin differences.

$$\frac{d}{dt}ReF = b\,FSH + [c_1\,FSH - c_2\,LH^{\alpha}]ReF, \tag{S5}$$

$$\frac{d}{dt}SeF = c_2\,LH^{\alpha}\,ReF + [c_3\,LH^{\beta} - c_4\,LH]SeF, \tag{S6}$$

$$\frac{d}{dt}PrF = c_4\,LH\,SeF - c_5\,LH^{\gamma}\,PrF, \tag{S7}$$

$$\frac{d}{dt}Ov_1 = c_5\,LH^{\gamma}\,PrF - d_1\,Ov_1, \tag{S8}$$

$$\frac{d}{dt}Ov_2 = d_1\,Ov_1 - d_2\,Ov_2, \tag{S9}$$

$$\frac{d}{dt}Lut_1 = d_2\,Ov_2 - k_1\,Lut_1, \tag{S10}$$

$$\frac{d}{dt}Lut_2 = k_1\,Lut_1 - k_2\,Lut_2, \tag{S11}$$

$$\frac{d}{dt}Lut_3 = k_2\,Lut_2 - k_3\,Lut_3, \tag{S12}$$

$$\frac{d}{dt}Lut_4 = k_3\,Lut_3 - k_4\,Lut_4. \tag{S13}$$

3. Effect of inhibin delay on model fit to data

Inhibin is a glycoprotein secreted by the ovaries and has a more complicated molecular structure than the steroids E_2 and P_4. It is well-known, e.g., see [10,33,41], that inhibin inhibits *FSH* synthesis. However, its mode of action has not been determined definitively but may involve competition with activin (which stimulates *FSH*) for the activin receptor or may bind with its own receptor [29]. Biological evidence indicates that this process of *FSH* suppression requires a significant time lag which is species-specific. For instance, it has been observed that, *in vitro*, inhibin suppresses *FSH* synthesis in bovine [10] and ovine [33] pituitary cells with a time lag of up to 72 h. *In vivo* experiments with rhesus monkeys by Ramaswamy et al. [26] reported *FSH* suppression with a time delay of about 48 h but, in rats, Robertson et al. [28] observed only a 4–8 h delay. In menstrual cycle "time-lagged analyses," Robertson et al. [30] computed a negative correlation between inhibin and *FSH* follicular phase data 72 h later. Our mathematical model requires an inhibin time delay of 36 h to obtain a very good approximation to the clinical data of Welt et al. [39]. This delay is consistent with current biological evidence and may suggest hypotheses for future biological experimentation.

System (A) and (S) with the inhibin delay has an asymptotically stable cycle of period 28 days instead of 26 days for the no-delay model [34]. The *LH* data indicates a 14 day follicular phase and the position and height of the *LH* surge for the delay model is consistent with that (see Fig. 1). Also, the delay E_2 follicular and luteal peaks are higher than E_2 for the no-delay model. To understand from a mathematical point of view why the inhibin delay is responsible for these differences we examine hormone profiles and ovarian stages for both models over three carefully chosen consecutive cycles. MATLAB simulations of both models were run with the following initial conditions (rounded to two decimal places) given in the order of the 13 state variables in (S), {29.65, 6.86, 8.47, 6.15, 3.83, 11.51, 5.48, 19.27, 45.64, 100.73, 125.95, 135.84, 168.71}. The simulations were aligned so that both delay and no-delay periodic orbits are as close to one another as possible at the beginning of their second cycle, indicated by the vertical line

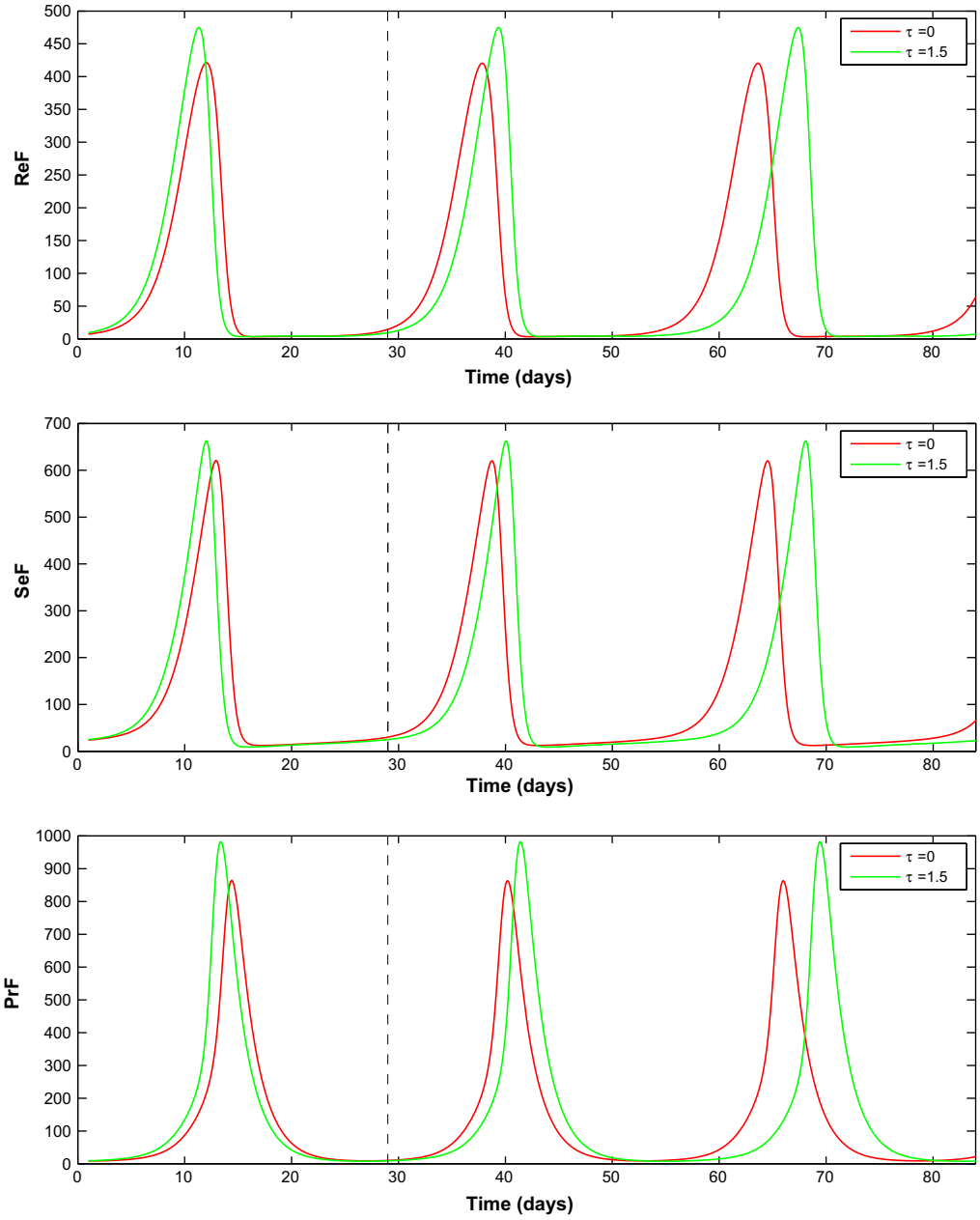

Fig. 3. First three ovarian stages *ReF*, *SeF* and *PrF* for three consecutive cycles of the delay model (green curves) and the no delay model (red curves). (For interpretation of the references to colour in this figure legend, the reader is referred to the web version of this article.)

at day 29 in Figs. 1–3. This was done so that the point of our comparison would be the second cycle in these figures and the preceding cycle would also be plotted because hormone profiles during the luteal phase of the preceding cycle influence behavior in our comparison cycle.

The key feature to observe in Fig. 2 is that the no-delay *FSH* (red curve) is higher than the delay *FSH* from day 19 until day 34, which includes the first six days of the follicular phase of our comparison cycle. Since *FSH* stimulates follicular development, the no-delay ovarian stages of the second cycle increase sooner than the delay ovarian stages and the no-delay cycle is advanced ahead of the delay cycle (see Fig. 3). No-delay *FSH* is higher because delay *Inh* has a greater inhibitory effect than no-delay *Inh* on *FSH* synthesis (see (S3)) during that period. Delay *Inh* (green curve) is greater than no-delay *Inh* from day 15 to day 22 where the curves cross and then both curves decrease in parallel until day 33.5. These *Inh* curves are so close to one another (see Fig. 2) from day 22 to day 33.5 that the delay of 1.5 days results in delay $Inh(t-1.5)$ being greater than no-delay $Inh(t)$ for this time interval. In fact, model simulations indicate that delay $Inh(t-1.5)$ is greater than no-delay $Inh(t)$ for $14.5 \leqslant t \leqslant 33.5$. Effectively, for this interval of 19 days, the synthesis of delay *FSH* is suppressed more than the synthesis of no delay *FSH*. This causes the no-delay follicles to develop sooner than the delay follicles with the consequence via (A1) that no-delay E_2 rises sooner (see Fig. 1). Since E_2 inhibits *FSH* release (see (S3-S4)), this earlier rise in E_2 tends to decrease no-delay *FSH* sooner than delay *FSH* with the result that the no-delay follicular stages develop to a lesser extent than the delay stages (Fig. 3). Also, because E_2 promotes *LH* synthesis, the *LH* surge is earlier and smaller for the no-delay model (Fig. 1). The cumulative effect of these profile differences is a shortening of the no-delay cycle length by 2 days and a reduction in no-delay hormone peaks.

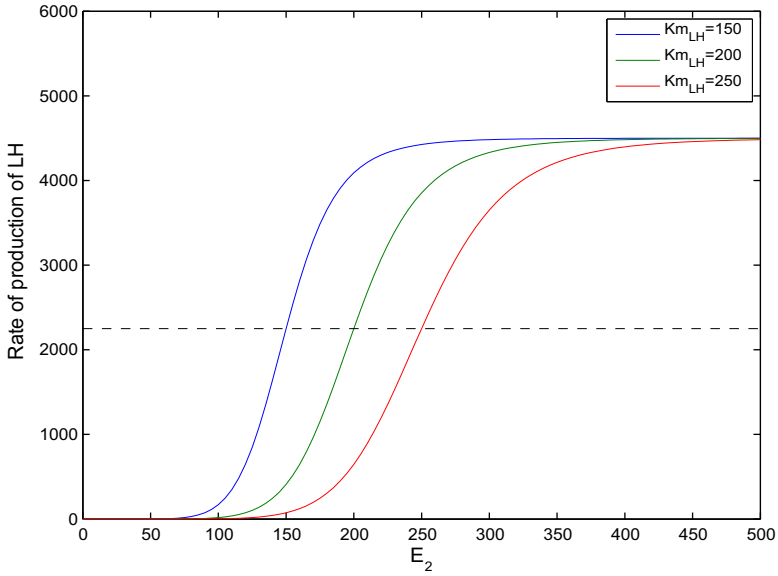

Fig. 4. Graphs of Hill functions, $\left(V_{1.LH}\ E_2^8\right)/\left(Km_{LH}^8 + E_2^8\right)$, for three values of Km_{LH}. The dashed line indicates the synthesis rate when $E_2 = Km_{LH}$, half-saturation.

Table 2
Size of cycle uniqueness interval for inhibin delay $\tau = 0$ (column 2) and $\tau = 1.5$ days (column 4) for increasing values of c_2. $c_2 = 0.07$ and $Km_{LH} = 200$ pg/mL give the best fit to data.

c_2	Size ($\tau = 0$)	Km_{LH} bounds ($\tau = 0$)	Size ($\tau = 1.5$)	Km_{LH} bounds ($\tau = 1.5$)
0.03	126	$147 < Km_{LH} < 273$	271	$40 < Km_{LH} < 311$
0.04	50	$181 < Km_{LH} < 231$	226	$44 < Km_{LH} < 270$
0.05	81	$153 < Km_{LH} < 234$	173	$85 < Km_{LH} < 258$
0.06	118	$122 < Km_{LH} < 230$	167	$80 < Km_{LH} < 247$
0.07	114	$98 < Km_{LH} < 212$	154	$73 < Km_{LH} < 227$
0.08	102	$84 < Km_{LH} < 186$	141	$63 < Km_{LH} < 204$

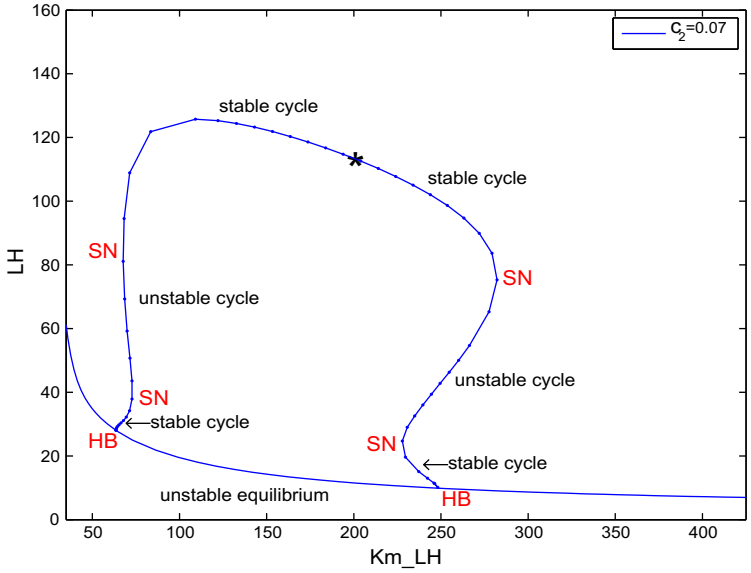

Fig. 5. In this bifurcation diagram the maximal *LH* value along a periodic solution or at an equilibrium is plotted against Km_{LH} when $\tau = 1.5$ and $c_2 = 0.07$. HB and SN denote Hopf and saddle-node bifurcations. The $*$ indicates the position of the cycle for the parameters of Table 1 and this cycle is the only stable solution at $Km_{LH} = 200$ pg/mL. The cycle uniqueness interval is the interval between the lower saddle-nodes, i.e., $73 < Km_{LH} < 227$.

A similar effect has been observed in older reproductive women, e.g., see Welt et al. [39], Klein et al. [18] and Hale et al. [12]. After age 35 a decrease in the number of follicles results in a decrease in inhibin and a consequential earlier follicular rise in *FSH* and E_2 and reduced cycle length as compared to younger women. Hence, the timing and serum concentration of inhibin appear to have significant effects on ovarian development during the follicular phase of the cycle.

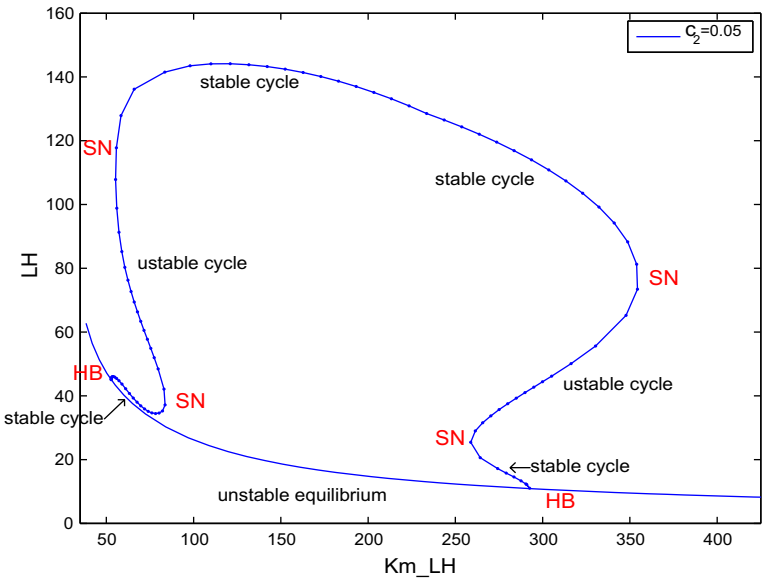

Fig. 6. Bifurcation diagram with respect to Km_{LH} when $\tau = 1.5$ and $c_2 = 0.05$. HB and SN denote Hopf and saddle-node bifurcations. The length of the cycle uniqueness interval is 173, i.e., $85 < Km_{LH} < 258$.

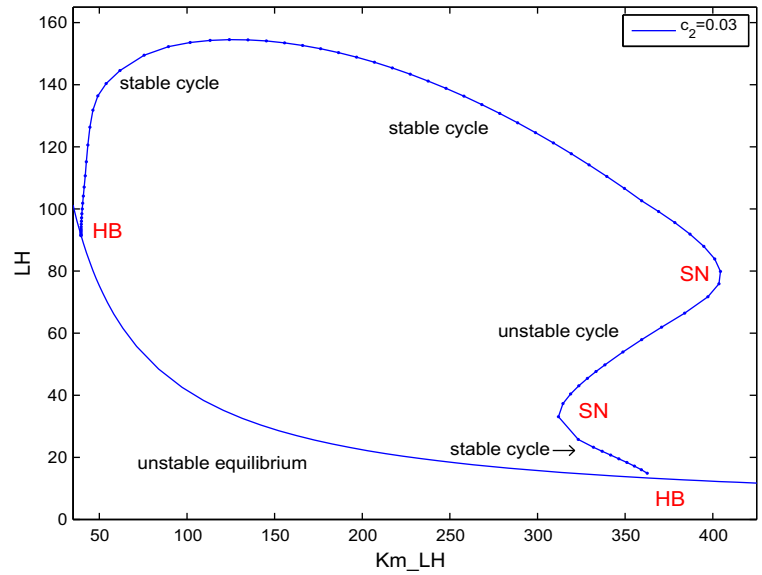

Fig. 7. Bifurcation diagram with respect to Km_{LH} when $\tau = 1.5$ and $c_2 = 0.03$. HB and SN denote Hopf and saddle-node bifurcations. The left hysteresis curve has disappeared and the length of the cycle uniqueness interval is 271, i.e., $40 < Km_{LH} < 311$.

4. Cycle uniqueness interval

The parameters Km_{LH} and c_2 are two of the three most sensitive parameters when sensitivity is measured with respect to the E_2 follicular peak as system output [24,35]. This E_2 peak is chosen as system output because a significant follicular E_2 level is necessary for the LH surge to occur. The parameter Km_{LH} is the half-saturation constant in the Hill function in (S1), $\left(V_{1,LH}\, E_2^8\right)/\left(Km_{LH}^8 + E_2^8\right)$. This sigmoidal shaped function (see Fig. 4) acts like a threshold for the synthesis of LH in response to E_2 blood levels. Once E_2 concentration reaches the value Km_{LH}, half way up the sigmoid as indicated by the dashed line in Fig. 4, then the pituitary is synthesizing LH in large amounts, which is necessary for ovulation. For larger values of Km_{LH}, E_2 must reach a higher level to produce the same LH synthesis rate. Because higher follicular E_2 levels may suggest a greater probability of abnormal cycling [34,35], we construct bifurcation diagrams where LH is plotted against the parameter Km_{LH} to determine the number of stable cycles for a given Km_{LH} value and to determine LH surge height along each cycle. When similar bifurcation diagrams were drawn for the no-delay model [34], an interval of Km_{LH} values was observed for which a unique stable periodic solution existed and it represented an ovulatory cycle. The length of this cycle uniqueness interval varied as the parameter c_2 was changed [34]. The present study reveals that these uniqueness intervals are larger for the model with inhibin delay, (A) and (S), as indicated in Table 2.

Here, the software DDEBIFTOOL [8] is used to construct bifurcation diagrams where the maximal LH value along a periodic solution or at a steady-state solution is plotted against the parameter Km_{LH}. Fig. 5 displays this bifurcation diagram where the remaining parameters are those in Table 1. Stable and unstable periodic orbits and equilibria are depicted. Saddle-node (SN) and Hopf (HB)

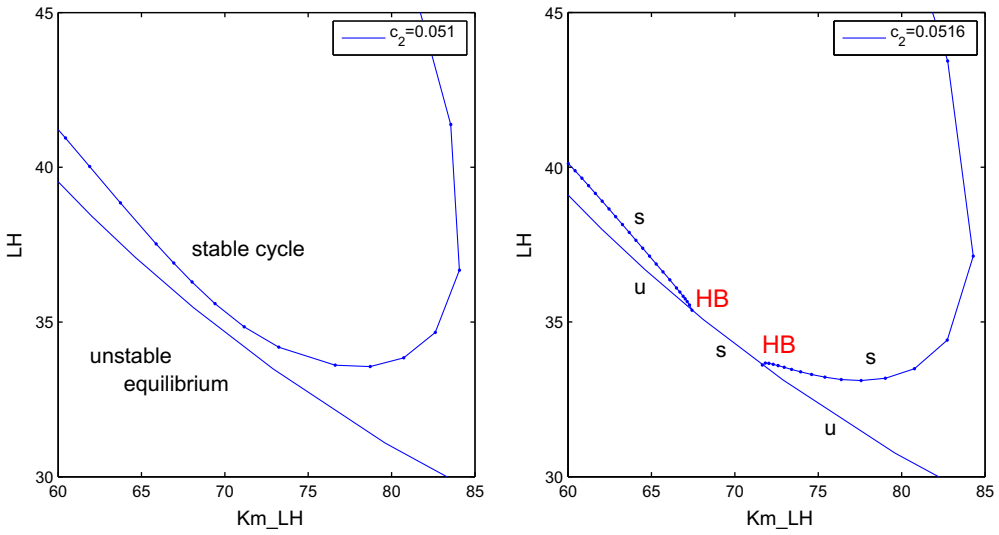

(a): Blow up for $c_2 = 0.051$ (b): Blow up for $c_2 = 0.0516$

Fig. 8. s indicates a stable and u, an unstable cycle or equilibrium. HB denotes a Hopf point.

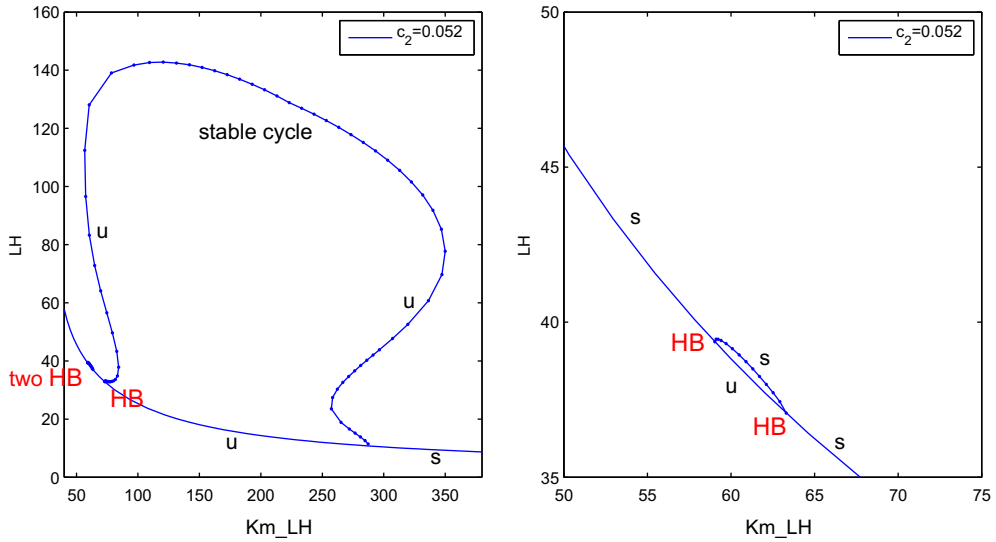

(a): $c_2 = 0.052$ (b): Blow up of "two HB" for $c_2 = 0.052$

Fig. 9. s indicates stable and u indicates unstable. HB denotes a Hopf point.

bifurcations are labeled. The curve along the lower portion of Fig. 5 tracks an equilibrium, which undergoes a supercritical Hopf bifurcation as Km_{LH} increases through 64 and another supercritical Hopf bifurcation at $Km_{LH} = 248$. The bifurcation at $Km_{LH} = 64$ results in a small amplitude, stable, periodic orbit which persists until $Km_{LH} = 73$. Stable and unstable cycles appear together at $Km_{LH} = 68$ via a saddle-node bifurcation of periodic orbits. The unstable orbit coalesces with the small amplitude stable Hopf orbit at $Km_{LH} = 73$ and both disappear in another saddle-node. The stable cycle appearing at $Km_{LH} = 68$ grows in amplitude, continues across the top portion of the diagram and disappears in a saddle-node at $Km_{LH} = 282$. This branch of periodic solutions represents the ovulatory cycles of the model (S) with (A), where the $*$ indicates the cycle corresponding to the Km_{LH} value of Table 1, 200 pg/ml. Analogous behavior occurs at the right side of the bifurcation diagram where the hysteresis character of the curve of periodic orbits is evident. Clearly, for Km_{LH} from 227 to 282 there is a stable, large amplitude ovulatory cycle and a stable, small amplitude non-ovulatory cycle or stable equilibrium. For Km_{LH} in the interval between the lower SN's in Fig. 5 ($73 < Km_{LH} < 227$), there is only one stable cycle and it is ovulatory. Selgrade [34] referred to this Km_{LH} interval as the cycle uniqueness interval. In the context of this cycle regulation model, a woman's Km_{LH} parameter must fall within her cycle uniqueness interval for her to be assured of only a normal cycle. From Fig. 5, we observe that decreasing Km_{LH} from 200 pg/mL keeps it within the interval and increases the height of the *LH* surge. However, increasing Km_{LH} to 227 moves Km_{LH} to a region of multiple stable cycles and possible non-ovulation. For $c_2 = 0.07$, the diameter of this cycle uniqueness interval is 154 for the delay model and only 114 for the no-delay model (see Table 2).

For the no-delay model, Selgrade [34] investigated how variations in the ovarian transfer parameter c_2 changed the size of the cycle uniqueness interval. Increasing c_2 from $c_2 = 0.07$ causes an increased transfer of mass from the first follicular stage *ReF* to the

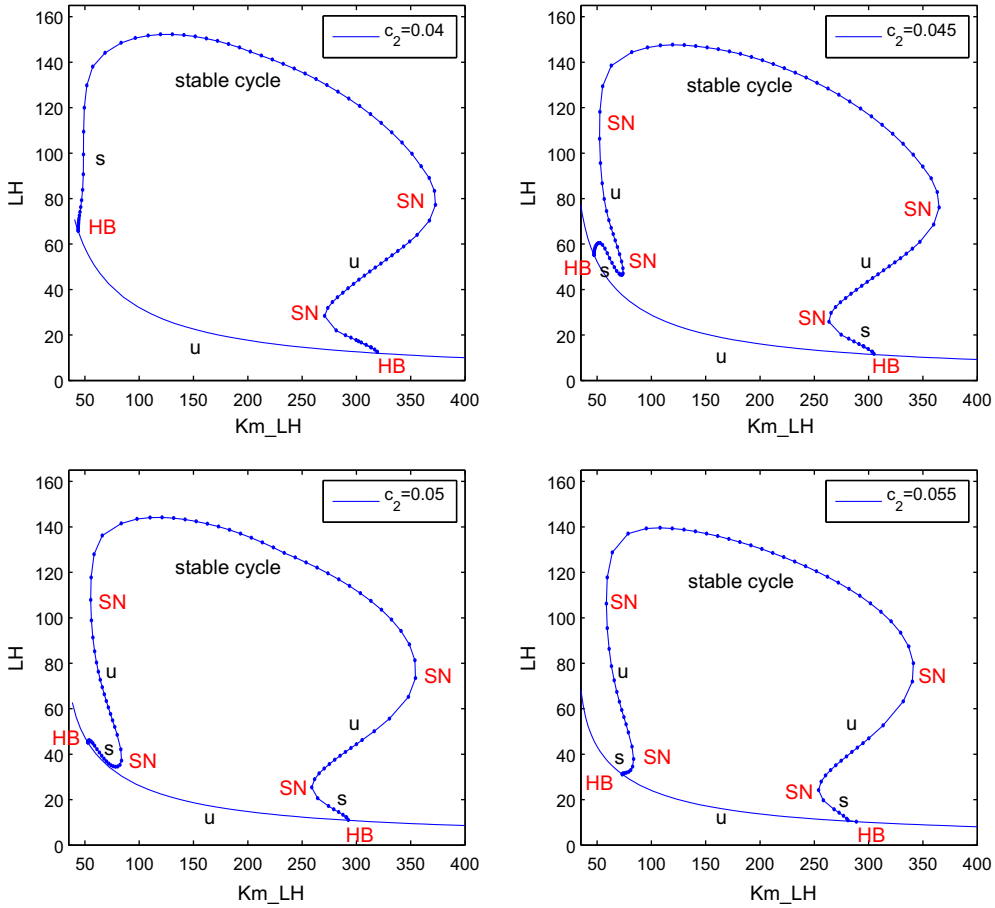

Fig. 10. Bifurcation diagrams with respect to Km_{LH} for $\tau = 1.5$ as c_2 increases from 0.04 to 0.055 by increments of 0.5. A kink appears in the large loop at the left and bends to touch the curve of equilibria causing a degenerate Hopf bifurcation. s indicates stable and u indicates unstable. <http://www4.ncsu.edu/~amargol/research/Fig10_Bif04to055.mpg> for an animated display of bifurcation diagrams as c_2 increases from 0.04 to 0.055 in increments of 0.001.

second stage *SeF* which diminishes the development of not only *ReF* but of all subsequent ovarian stages. Effectively, ovarian hormone production is reduced and the cycle uniqueness interval is decreased for both delay and no-delay models. For a biological interpretation, we conjecture that too large a c_2 parameter stunts the growth of small recruited follicles and results in diminished ovarian mass during the follicular phase. However, ovulation may still occur. Table 2 lists the cycle uniqueness intervals for various values of c_2 which we compute for the delay model ($\tau = 1.5$) and which were reported in [34] for the no-delay model ($\tau = 0$). Decreasing c_2 from 0.07 in increments of 0.01 widens the cycle uniqueness interval for the delay model but shrinks it for the no-delay model until $c_2 = 0.03$. This is an important difference between the delay and the no-delay models and indicates a certain amount of biological inexplicability in the no-delay model. Mathematically, for the no-delay model as c_2 decreases, the cycle uniqueness interval shrinks because the hysteresis curves enlarge and the Hopf points move closer together resulting in a narrowing of the gap between the lower two saddle-nodes. Then, as described in [34], an unfolding of a transcritical bifurcation occurs as c_2 decreases through 0.0305 and this results in the disappearance of the left hysteresis curve and a rapid expansion of the cycle uniqueness interval (see Table 2 for $\tau = 0$, $c_2 = 0.04$ and $c_2 = 0.03$). In contrast, for the delay model, decreasing c_2 from 0.07 causes the hysteresis curves to enlarge only slightly (compare Figs. 5 and 6) and the Hopf points to move apart. Instead of disappearing due to a transcritical bifurcation, the left hysteresis curve in the delay bifurcation diagram disappears due to two degenerate Hopf bifurcations described below. The uniqueness interval for $\tau = 1.5$ when $c_2 = 0.03$ (Fig. 7) is over twice as large as that for the no-delay model. The inhibin delay ($\tau = 1.5$) and the additional growth of the first follicular stage (smaller c_2) result in a large interval of Km_{LH} values where there is a unique ovulatory menstrual cycle.

The broad expansion of the cycle uniqueness interval for c_2 less than 0.05 is due to two different unfoldings of degenerate Hopf bifurcations which occur for c_2 near 0.05. Each Hopf bifurcation is degenerate because the real part of the eigenvalue pair crossing the imaginary axis has a zero derivative with respect to the parameter at crossing. One of these degeneracies occurs when two Hopf points coalesce at $c_2 = 0.05147$ and $Km_{LH} = 69.8458$. At $c_2 = 0.05$, the left side of Fig. 6 displays a branch of stable cycles lying just above a branch of unstable equilibria. Fig. 8(a) blows these curves up at $c_2 = 0.051$. They touch when $c_2 = 0.05147$ producing a degenerate Hopf point. Then as c_2 increases, the degenerate Hopf point separates into two non-degenerate, supercritical Hopf points with stable equilibria in between them pictured at $c_2 = 0.0516$ in Fig. 8(b). As discussed in Golubitsky and Schaeffer [11, p. 375] , the unfolding of this bifurcation may be described roughly by the equation

$$-x^3 + (Km_{LH} - 69.8458)^2 x + (0.05147 - c_2)x = 0, \qquad \text{(DegHB1)}$$

where x represents the state variable *LH* and the line $\{x = 0\}$ represents the curve of equilibria. As c_2 continues to increase above 0.052, the two Hopf points on the left in Fig. 9(a) coalesce in a second degenerate Hopf point at $c_2 = 0.05209$ and $Km_{LH} = 61.0174$ and

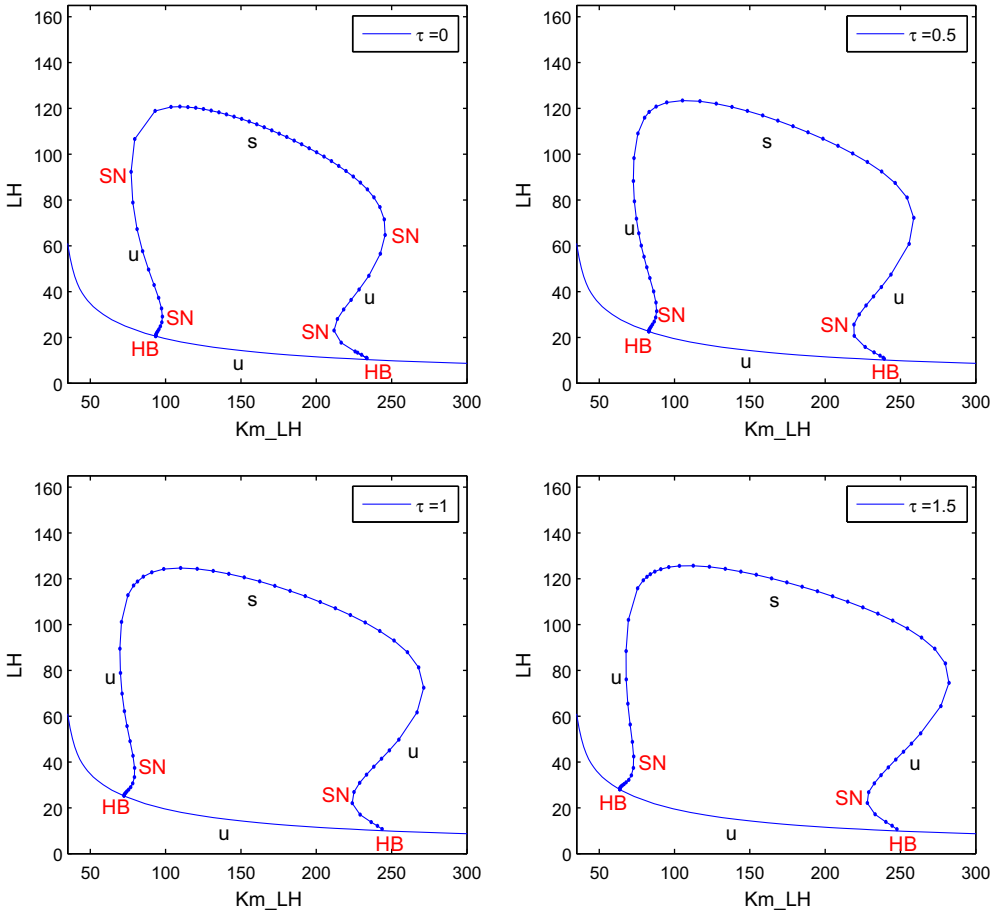

Fig. 11. Bifurcation diagrams with respect to Km_{LH} for $c_2 = 0.07$ as τ increases from $\tau = 0$ to $\tau = 1.5$ by increments of 0.5. The cycle uniqueness interval enlarges from 114 to 154. HB and SN denote Hopf and saddle-node bifurcations. s indicates a stable and u, an unstable cycle or equilibrium.

that Hopf point disappears for $c_2 > 0.05209$. The unfolding of this bifurcation may be represented by the equation (see [11])

$$x^3 + (Km_{LH} - 61.0174)^2 x + (c_2 - 0.05209)x = 0. \qquad \text{(DegHB2)}$$

As c_2 increases above 0.05209, the saddle-nodes which determine the cycle uniqueness interval move closer together causing the interval to shrink and move to the left, see Table 2.

As c_2 increases from 0.04 to 0.045, the left hysteresis curve forms because of the appearance of a kink and two saddle-nodes along the left edge of the large loop of periodic solutions (Fig. 10). This kink and the two degenerate Hopf unfoldings (DegHB1 and DegHB2) are embedded in the continuous display of bifurcation diagrams as c_2 increases from 0.04 to 0.055, see Fig. 10.

5. Comparing bifurcation diagrams as delay τ varies

For all c_2 values in Table 2, the delay model has a larger cycle uniqueness interval than the no-delay model. As discussed previously, when $Km_{LH} = 200$ and $c_2 = 0.07$ the delay in the effect of inhibin on *FSH* results in more vigorous growth of ovarian stages, a longer cycle and higher hormone peaks. Numerical simulations indicate that this is also true after reasonable variations in both model parameters, Km_{LH} and c_2. It is conceivable that the more robust ovarian development of the delay model permits a broader range of half-saturation constants Km_{LH} for the successful surge response of *LH* to E_2 priming and, hence, a larger cycle uniqueness interval. Bifurcation diagrams for various values of τ support this suggestion.

First we fix $c_2 = 0.07$, which is the parameter value fitting the data best (see Table 1). We draw bifurcation diagrams with respect to Km_{LH} to study how the cycle uniqueness interval opens up as the delay τ increase from 0 to 1.5. Fig. 11 illustrates these diagrams for τ values increasing from $\tau = 0$ to $\tau = 1.5$ by increments of 0.5. As τ increases the Hopf points (HB) along the curve of equilibria spread apart as do the saddle-nodes (SN), which determine the cycle uniqueness interval. The qualitative features of these diagrams are similar. In particular, there are hysteresis curves on both the left and right edges of a large loop of periodic solutions. The hysteresis curves give rise to two regions of periodic bistability.

For other values of c_2, these two hysteresis curves do not persist for all values of τ. For instance, if $c_2 = 0.04$ then the hysteresis curve on the left disappears as τ increases. The cycle uniqueness interval enlarges from 50 when $\tau = 0$ to 226 when $\tau = 1.5$. The primary reason for this drastic increase is a sequence of bifurcations that occur as τ increases from 0.7 to 1.2. A degenerate Hopf bifurcation similar to that described by (DegHB2) occurs at $\tau = 0.73$ resulting in a bump of stable cycles to the left of the large loop of periodic solutions as pictured in Fig. 12. This Hopf bump of stable solutions is just below the branch of unstable cycles in the left hysteresis curve and, as τ increases, this bump grows and touches the curve of cycles above producing a transcritical bifurcation of periodic solutions in the parameter Km_{LH} when $\tau = 1.06$. The unfolding of this transcritical bifurcation is analogous to that discussed in [34] except here the second parameter is τ instead of c_2. For τ values just above 1.06 the bump of stable cycles appears on the other side of the large loop of cycles (see Fig. 12) and disappears via the following sequence of bifurcations. At $\tau = 1.11$ a degenerate Hopf

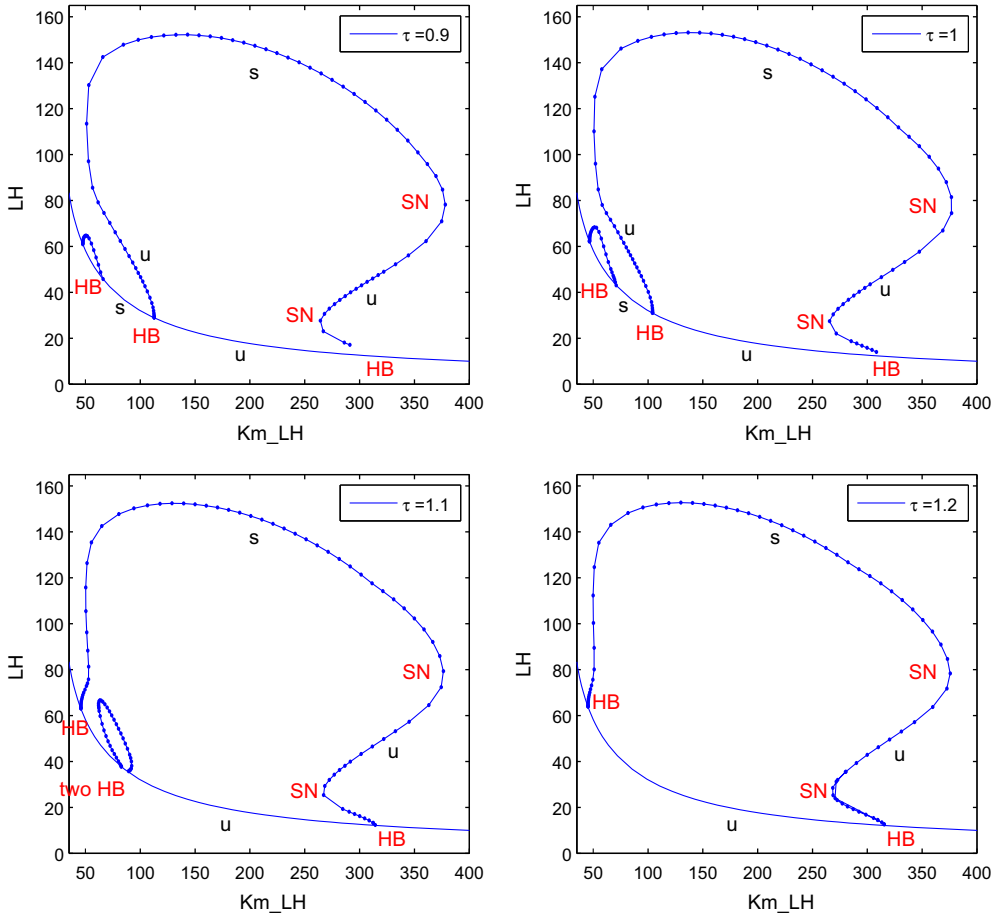

Fig. 12. Bifurcation diagrams with respect to Km_{LH} for $c_2 = 0.04$ as τ increases from $\tau = 0.9$ to $\tau = 1.2$ by increments of 0.1. HB and SN denote Hopf and saddle-node bifurcations. s indicates a stable and u, an unstable cycle or equilibrium. <http://www4.ncsu.edu/~amargol/research/Fig12_Bif04.mpg> for an animated display of transcritical and degenerate Hopf bifurcations as τ increasing from 0.7 to 1.2 in increments of 0.02.

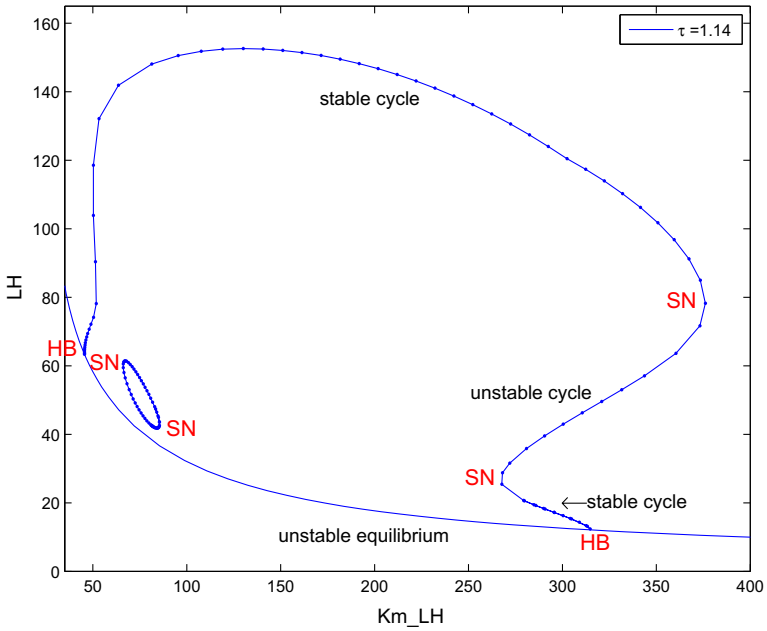

Fig. 13. Bifurcation diagram with respect to Km_{LH} when $\tau = 1.14$ and $c_2 = 0.04$. HB and SN denote Hopf and saddle-node bifurcations. The small closed loop of cycles has saddle-nodes at each end.

bifurcation like (DegHB1) causes the Hopf bump to separate from the curve of equilibria producing a small closed loop of periodic solutions (Fig. 13). Then this loop shrinks and disappears because the two saddle-nodes at each end of the loop coalesce and annihilate

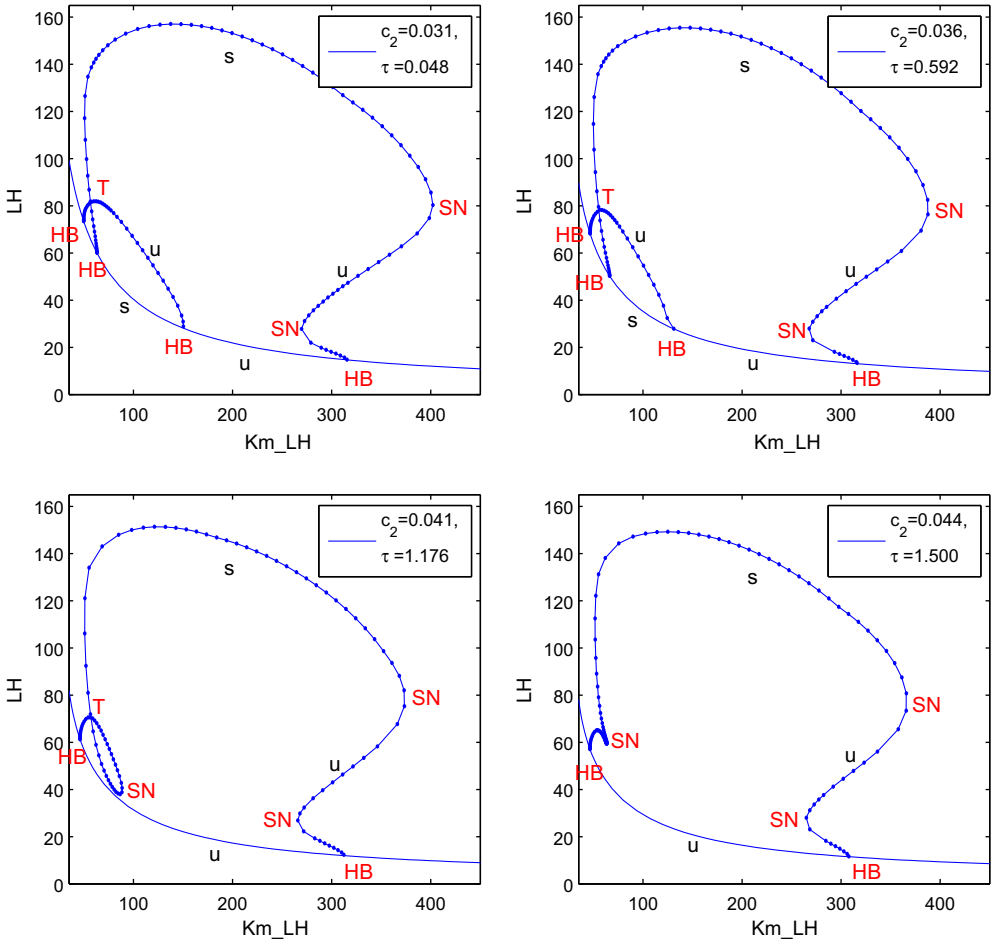

Fig. 14. Bifurcation diagrams with respect to Km_{LH} as τ increases from 0.048 to 1.5 and c_2 increases from 0.031 to 0.044. HB, SN and T denote Hopf, saddle-node and transcritical bifurcations. s indicates a stable and u, an unstable cycle or equilibrium. <http://www4.ncsu.edu/~amargol/research/Fig14_trans.mpg> for an animated display of a sequence of transcritical bifurcations revealing the creation of a loop and the broadening of the cycle uniqueness interval as τ and c_2 increase.

one another at $\tau = 1.173$. The unfolding of these bifurcations as τ increases from 0.7 to 1.2 is animated in Fig. 12.

The transcritical bifurcation is a prominent feature of the left side of the bifurcation diagrams for smaller values of τ. When this bifurcation is present in the diagram, the cycle uniqueness interval has reduced length, e.g., only 125 for the first frame of Fig. 14. The transcritical bifurcation persists for the parameter pairings in Fig. 14 until the transcritical bifurcation point coalesces with a saddle-node for $\tau \approx 1.45$. As τ increases, the cycle uniqueness interval grows although c_2 is also increasing (see the animation for Fig. 14). Hence, a larger delay in the effect of inhibin may compensate for an apparent reduction in growth of the first follicular stage of a cycle. In fact, an increase in *FSH* inhibition during the luteal phase of the previous cycle due to the delay in inhibin results in greater early follicular development during the next cycle (see the middle cycle in Fig. 3).

6. Summary and conclusion

The half-saturation parameter Km_{LH} in the Hill function in (S1) indicates the level of E_2 sufficient for significant *LH* synthesis. We study bifurcation diagrams where maximum *LH* along a periodic or equilibrium solution is graphed against Km_{LH}. We observe an interval of Km_{LH} values for which the model admits a unique stable periodic solution and this solution represents an ovulatory cycle. A large cycle uniqueness interval signifies a wide range of follicular E_2 levels which promote a *LH* surge sufficient for ovulation. This cycle uniqueness interval is usually determined by two saddle-node bifurcations which lie on hysteresis curves at the left and right sides of the bifurcation diagram.

The parameter τ is the time delay for the inhibition of *FSH* synthesis caused by inhibin. In Section 3, we explain why a delay of 1.5 days (the value of τ fitting the data best) is consistent with biological evidence and permits increased ovarian development during the follicular phase of the cycle and a larger interval of Km_{LH} values which result in a unique cycle. The ovarian growth parameter c_2 promotes mass transfer between the first two stages of ovarian development and is indicative of healthy follicular growth. For various values of c_2, we illustrate how the cycle uniqueness interval grows as τ increases due to the occurrences of transcritical and degenerate Hopf bifurcations, e.g., see Fig. 12. Also, for delay τ near 1.5 days, Section 4 asserts that the cycle uniqueness interval increases as c_2 decreases because of additional growth of the first follicular stage, which represents small antral follicles.

Model simulations and bifurcation diagrams studied here imply that parameter combinations which provide for the sustained growth of small antral follicles at the beginning of the cycle may result in a greater possibility of normal cycling.

Acknowledgments

The authors thank Georgina E. Hale, Claude L. Hughes and an anonymous reviewer for helpful conversations and suggestions which improved the paper.

Appendix A. Supplementary data

Supplementary data associated with this article can be found, in the online version, at doi:10.1016/j.mbs.2011.09.001.

References

[1] F. Alvarez-Blasco, J.I. Botella-Carretero, J.L. San Millan, H.F. Escobar-Morreale, Prevalence and characteristics of the polycystic ovary syndrome in overweight and obese women, Arch. Intern. Med. 166 (2006) 2081.

[2] R. Azziz, K.S. Woods, R. Reyna, T.J. Key, E.S. Knochenhauser, B.O. Yildiz, The prevalence and features of the polycystic ovary syndrome in an unselected population, J. Clin. Endocrinol. Metab. 89 (2004) 2745.

[3] H.M.T. Boer, C. Stötzel, S. Röblitz, P. Deuflhard, R.F. Veerkamp, H. Woelders, A simple mathematical model of the bovine estrous cycle: follicle development and endocrine interactions, J. Theor. Biol. 278 (2011) 20.

[4] R.J. Bogumil, M. Ferin, J. Rootenberg, L. Speroff, R.L. Vande Wiele, Mathematical studies of the human menstrual cycle. I: Formulation of a mathematical model, J. Clin. Endocrinol. Metab. 35 (1972) 126.

[5] R.J. Bogumil, M. Ferin, R.L. Vande Wiele, Mathematical studies of the human menstrual cycle. II: Simulation performance of a model of the human menstrual cycle, J. Clin. Endocrinol. Metab. 35 (1972) 144.

[6] G.N. Derry, P.S. Derry, Characterization of chaotic dynamics in the human menstrual cycle, Nonlinear Biomed. Phys. 4 (2010) 5.

[7] E.J. Doedel, AUTO: a program for the automatic bifurcation analysis of autonomous systems, Congr. Numer. 30 (1981) 265.

[8] K. Engelborghs, T. Luzyanina, D. Roose, Numerical bifurcation analysis of delay differential equations, J. Comput. Appl. Math. 125 (2000) 265.

[9] B. Ermentrout, Simulating, Analyzing, and Animating Dynamical Systems, SIAM, Philadelphia, PA, 2002.

[10] P. Franchimont, K. Henderson, G. Verhoeven, M.T. Hazee-Hagelstein, C. Charlet-Renard, A. Demoulin, J.P. Bourguignon, M.J. Lecomte-Yerna, Inhibin: mechanisms of action and secretion, in: P. Franchimont, C.P. Channing (Eds.), Intragonadal Regulation of Reproduction, Academic Press, London, 1981, p. 167.

[11] M. Golubitsky, D.G. Schaeffer, Singularities and Groups in Bifurcation Theory, vol. 1, Springer-Verlag, New York, 1985.

[12] G.E. Hale, X. Zhao, C.L. Hughes, H.G. Burger, D.M. Robertson, I.S. Fraser, Endocrine features of menstrual cycles in middle and late reproductive age and the menopausal transition classified according to the staging of reproductive aging workshop (STRAW) staging system, J. Clin. Endocrinol. Metab. 92 (2007) 3060.

[13] L.A. Harris, Differential Equation Models for The Hormonal Regulation of The Menstrual Cycle, Ph.D. Thesis, North Carolina State University, Raleigh, North Carolina, 2001. <www.lib.ncsu.edu/theses/available/etd-04222002-153727/unrestricted/etd.pdf>.

[14] L. Harris-Clark, P.M. Schlosser, J.F. Selgrade, Multiple stable periodic solutions in a model for hormonal control of the menstrual cycle, Bull. Math. Biol. 65 (2003) 157.

[15] J. Hotchkiss, E. Knobil, The menstrual cycle and its neuroendocrine control, in: E. Knobil, J.D. Neill (Eds.), The Physiology of Reproduction, second ed., Raven Press, Ltd., New York, 1994, p. 711.

[16] F.J. Karsch, D.J. Dierschke, R.F. Weick, T. Yamaji, J. Hotchkiss, E. Knobil, Positive and negative feedback control by estrogen of luteinizing hormone secretion in the rhesus monkey, Endocrinology 92 (1973) 799.

[17] J. Keener, J. Sneyd, Mathematical Physiology I: Cellular Physiology, second ed., Springer-Verlag, New York, 2009.

[18] N.A. Klein, A.J. Harper, B.S. Houmard, P.M. Sluss, M.R. Soules, Is the short follicular phase in older women secondary to advanced or accelerated dominant follicle development?, J Clin. Endocrinol. Metab. 87 (2002) 5746.

[19] J.H. Liu, S.S.C. Yen, Induction of midcycle gonadotropin surge by ovarian steroids in women: a critical evaluation, J. Clin. Endocrinol. Metab. 57 (1983) 797.

[20] J.E.A. McIntosh, R.P. McIntosh, Mathematical Modeling and Computers in Endocrinology, Springer-Verlag, Berlin, 1980.

[21] R.I. McLachlan, N.L. Cohen, K.D. Dahl, W.J. Bremner, M.R. Soules, Serum inhibin levels during the periovulatory interval in normal women: relationships with sex steroid and gonadotrophin levels, Clin. Endocrinol. 32 (1990) 39.

[22] W.D. Odell, The reproductive system in women, in: L.J. DeGroot (Ed.), Endocrinology, Grune & Stratton, New York, 1979, p. 1383.

[23] S.R. Ojeda, Female reproductive function, in: J.E. Griffin, S.R. Ojeda (Eds.), Textbook of Endocrine Physiology, second ed., Oxford University, Oxford, 1992, p. 134.

[24] R.D. Pasteur, A Multiple-inhibin Model for the Human Menstrual Cycle, Ph.D. Thesis, North Carolina State University, Raleigh, North Carolina, 2008. <http://www.lib.ncsu.edu/theses/available/etd-06102008-194807/>.

[25] L. Plouffe Jr., S.N. Luxenberg, Biological modeling on a microcomputer using standard spreadsheet and equation solver programs: the hypothalamic–pituitary–ovarian axis as an example, Comput. Biomed. Res. 25 (1992) 117.

[26] S. Ramaswamy, C.R. Pohl, A.S. McNeilly, S.J. Winters, T.M. Plant, The time course of follicle-stimulating hormone suppression by recombinant human inhibin A in the adult rhesus monkey, Endocrinology 139 (1998) 3409.

[27] I. Reinecke, P. Deuflhard, A complex mathematical model of the human menstrual cycle, J. Theor. Biol. 247 (2007) 303.

[28] D.M. Robertson, M. Prisk, J.W. McMaster, D.C. Irby, J.K. Findlay, D.M. de Kretser, Serum FSH-suppressing activity of human recombinant inhibin A in male and female rats, J. Reprod. Fertil. 91 (1991) 321.

[29] D.M. Robertson, R. Hertan, P.G. Farnworth, Is the action of inhibin mediated via a unique receptor?, Rev Reprod. 5 (2000) 131.

[30] D.M. Robertson, G.E. Hale, D. Jolley, I.S. Fraser, C.L. Hughes, H.G. Burger, Interrelationships between ovarian and pituitary hormones in ovulatory menstrual cycles across reproductive age, J. Clin. Endocrinol. Metab. 94 (2009) 138.

[31] R.C. Robinson, An Introduction to Dynamical Systems: Continuous and Discrete, Pearson Prentice Hall, New Jersey, 2004.

[32] P.M. Schlosser, J.F. Selgrade, A model of gonadotropin regulation during the menstrual cycle in women: qualitative features, Environ. Health Perspect. 108 (Suppl. 5) (2000) 873.

[33] R.S. Scott, H.G. Burger, Mechanism of action of inhibin, Biol. Reprod. 24 (1981) 541.

[34] J.F. Selgrade, Bifurcation analysis of a model for hormonal regulation of the menstrual cycle, Math. Biosci. 225 (2010) 108.

[35] J.F. Selgrade, L.A. Harris, R.D. Pasteur, A model for hormonal control of the menstrual cycle: structural consistency but sensitivity with regard to data, J. Theor. Biol. 260 (2009) 572.

[36] J.F. Selgrade, P.M. Schlosser, A model for the production of ovarian hormones during the menstrual cycle, Fields Inst. Commun. 21 (1999) 429.

[37] A.E. Treloar, R.E. Boynton, B.G. Behn, B.W. Brown, Variation of the human menstrual cycle through reproductive life, Int. J. Fertil. 12 (1967) 77.

[38] C.F. Wang, B.L. Lasley, A. Lein, S.S.C. Yen, The functional changes of the pituitary gonadotrophs during the menstrual cycle, J. Clin. Endocrinol. Metab. 42 (1976) 718.

[39] C.K. Welt, D.J. McNicholl, A.E. Taylor, J.E. Hall, Female reproductive aging is marked by decreased secretion of dimeric inhibin, J. Clin. Endocrinol. Metab. 84 (1999) 105.

[40] S.S.C. Yen, Polycystic ovarian syndrome (hyperandrogenic chronic anovulation), in: S.S.C. Yen, R.B. Jaffe, R.L. Barbieri (Eds.), Reproductive Endocrinology. Physiology, Pathophysiology and Clinical Management, fourth ed., W.B. Saunders Co., Philadelphia, 1999, p. 436.

[41] S.S.C. Yen, The human menstrual cycle: neuroendocrine regulation, in: S.S.C. Yen, R.B. Jaffe, R.L. Barbieri (Eds.), Reproductive Endocrinology. Physiology, Pathophysiology and Clinical Management, fourth ed., W.B. Saunders Co., Philadelphia, 1999, p. 191.

[42] A.J. Zeleznik, D.F. Benyo, Control of follicular development, corpus luteum function, and the recognition of pregnancy in higher primates, in: E. Knobil, J.D. Neill (Eds.), The Physiology of Reproduction, second ed., Raven Press, Ltd., New York, 1994, p. 751.